Inhibitors can arrest the membrane activity of human islet amyloid polypeptide independently of amyloid formation

FEBS Letters 507 (2001) 200–204 FEBS 25366

Inhibitors can arrest the membrane activity of human islet amyloid polypeptide independently of amyloid formation

Thad A. Harroun[a], Jeremy P. Bradshaw[a], Richard H. Ashley[b,*]

[a] *Department of Preclinical Veterinary Sciences, University of Edinburgh, George Square, Edinburgh EH8 9XD, UK*
[b] *Department of Biomedical Sciences, University of Edinburgh, George Square, Edinburgh EH8 9XD, UK*

Received 17 September 2001; accepted 26 September 2001

First published online 9 October 2001

Edited by Jacques Hanoune

Abstract Human islet amyloid polypeptide (hIAPP), co-secreted with insulin from pancreatic β cells, misfolds to form amyloid deposits in non-insulin-dependent diabetes mellitus (NIDDM). Like many amyloidogenic proteins, hIAPP is membrane-active: this may be significant in the pathogenesis of NIDDM. Non-fibrillar hIAPP induces electrical and physical breakdown in planar lipid bilayers, and IAPP inserts spontaneously into lipid monolayers, markedly increasing their surface area and producing Brewster angle microscopy reflectance changes. Congo red inhibits these activities, and they are completely arrested by rifampicin, despite continued amyloid formation. Our results support the idea that non-fibrillar IAPP is membrane-active, and may have implications for therapy and for structural studies of membrane-active amyloid.

Key words: Brewster angle microscopy; Congo red; Langmuir film; Diabetes mellitus; Planar lipid bilayer; Rifampicin

1. Introduction

Many human and animal diseases, including Alzheimer's disease (AD) and non-insulin-dependent diabetes mellitus (NIDDM), are characterised by the presence of 'amyloid' in affected tissues. Amyloid is composed of misfolded β-sheet rich proteins that assemble spontaneously into protofibrils which subsequently form higher order structures, ranging from simple twisted pairs of helical fibrils to complex and extensive sheets of protein [1]. Although different cellular proteins misfold in particular diseases, for example neuronal Aβ proteins in AD, and pancreatic β cell islet amyloid polypeptide (IAPP) in NIDDM, protofibrils share a common structure that confers distinctive physical properties shared by all amyloid deposits. These properties include diagnostic green birefringence under crossed polarisers in the presence of the histological stain Congo red, attributable to the characteristic 'cross β' structure of the fibrils [2–4].

The amyloidogenic protein IAPP (also known as amylin), a 37 residue polypeptide hormone co-secreted with insulin, has been directly implicated in the pathogenesis of NIDDM because (a) IAPP is normally soluble, and only misfolds and aggregates in NIDDM, and (b) there is a strong correlation between the ability of IAPPs from different mammals to form amyloid, and susceptibility to NIDDM. For example, humans and cats can develop NIDDM, and if they do, their IAPPs form amyloid in and around pancreatic islet cells. Rat and mouse IAPPs do not have an amyloidogenic motif [5,6] and these animals do not develop NIDDM. Consistent with these observations, recombinant human (h) IAPP is both amyloidogenic and membrane-active in cells transfected with appropriate cDNAs, and mice expressing the hIAPP transgene can develop a condition closely resembling NIDDM [7].

In vitro, hIAPP misfolds and aggregates spontaneously, whereas in individuals with NIDDM, IAPP presumably only misfolds after evading normal processing. The primary defect, which may result from a combination of inherited and environmental factors, remains to be discovered. In any case, misfolded IAPP is demonstrably toxic to cells. At the membrane level, misfolded IAPP interacts with lipid bilayers to destabilise them, and forms poorly selective cation-permeable 'ion channels' [8]. In vivo, similar effects could result in excessive Ca^{2+} entry and cell death, and increases in intracellular [Ca^{2+}] secondary to the loss of plasma membrane integrity may be augmented by the disruption of membrane-bound stores by intracellular amyloid. The availability of multiple mechanisms, with different rates and modes of Ca^{2+} entry into the cytoplasm, could help to explain why cells exposed to amyloidogenic IAPP die by both apoptosis and necrosis [9]. In contrast, a non-aggregating form of IAPP (rat IAPP) does not destabilise planar bilayers, and hIAPP that has been allowed to develop fibrils is also inert [9]. A similar observation has been made concerning Aβ proteins [10]. The membrane activity of IAPP thus appears to be related to the presence of an early, transitory, molecular form [9], distinct from the fibrillar IAPP found in mature amyloid.

The 'toxicity' of IAPP and Aβ proteins is reduced by rifampicin and related chemicals [11,12], and also by Congo red [13,14]. In the present study, we show that rifampicin and Congo red inhibit the membrane activity of freshly dissolved non-fibrillar hIAPP, although the protein continues to aggregate and form amyloid. In addition, we show that rifampicin prevents membrane insertion of the peptide. Our results provide an independent test of the hypothesis that an early, non-fibrillar form of IAPP is membrane-active [9]. We also provide a method to arrest the membrane activity of IAPP before irreversible membrane breakdown occurs. The use of similar inhibitors may allow more detailed structural studies of the molecular basis of the membrane activity of amyloid proteins, and new ways to intervene in amyloid diseases.

*Corresponding author. Fax: (44)-131-650 3711.
E-mail address: richard.ashley@ed.ac.uk (R.H. Ashley).

0014-5793/01/$20.00
PII: S0014-5793(01)02972-6

2. Materials and methods

2.1. Materials

hIAPP was synthesised by Bachem (St Helens, UK) and ResGen (Huntsville, AL, USA). The peptide was stored desiccated at −20°C. Rifampicin was from Fluka (Poole, UK) and Congo red was obtained from Sigma (Poole, UK). Freshly dissolved synthetic hIAPP was confirmed to be monomeric by light-scattering studies, as in previous work [9], and we also confirmed the absence of fibrils following negative staining and electron microscopy. Dimyristoyl-phosphatidylcholine (DMPC), palmitoyloleoyl-phosphatidylethanolamine (POPE) and palmitoyloleoyl-phosphatidylserine (POPS) were purchased from Avanti (Birmingham, AL, USA), and used without further purification.

2.2. Planar bilayer recording

Planar bilayers were cast across a 0.3 mm diameter hole in a polystyrene partition separating two solution-filled chambers. The experiments were carried out at room temperature in 10 mM KCl buffered with 20 mM Tris–HCl (pH 7.4), using bilayers cast from equimolar mixtures of POPE and POPS suspended in decane, as previously described [9,15]. Bilayer currents were digitally recorded under voltage-clamp conditions using an Axopatch 200B amplifier (Axon, Foster City, CA, USA). All values for voltage and current were measured with reference to the *cis* chamber, and the *trans* chamber was grounded. Large, high-resistance bilayer membranes, with a capacitance of at least 200 pF and a conductance less than 5 pS (i.e. less than 25 pS/nF), were observed for 14 min before use, to verify that they were electrically stable. IAPP was added to the bilayers by stirring small aliquots (~1% (v/v)) of freshly dissolved concentrated solutions into the *cis* chamber, using a magnetic stirrer. Salt concentrations were altered by additions from concentrated stock solutions, or by perfusion (10 volumes). Inhibitors were added as small (~1% (v/v)) aliquots of concentrated stock solutions (up to 20 mM), as described in Section 3.

2.3. Langmuir films

Lipid monolayers were assembled using a Langmuir film balance (NIMA Technology, Coventry, UK) with a surface pressure feedback system to measure the area per lipid molecule (i.e. monolayer expansion or contraction) at constant surface pressure. IAPP and inhibitors were added to the subphase as required. A pure water isotherm was recorded before each experiment to confirm the absence of residual surface impurities. Lipids were then deposited directly onto the surface from chloroform dispersions, with the trough barrier open to its maximum position. The solvent was allowed to evaporate unperturbed for 15 min, and a further compression isotherm was recorded to verify that the lipid monolayer remained free from impurities. Typically, no more than 30 μg of lipid was used to form the monolayer, in order to restrict the final surface area to no more than 20–25% of the maximum area available (~200 cm^2). This allowed for any expansion following incorporation of the peptide. The surface pressure was then set to 18–20 mN/m, to provide an area of 65 $Å^2$ per molecule of pure lipid. After constructing a lipid monolayer, IAPP was dissolved in purified water and immediately transferred to the subphase by pipetting the solution underneath the trough barrier, to provide a final subphase concentration of 5 μM. The barrier movement was programmed to maintain the initial surface pressure, and we recorded any changes in surface area. In experiments with inhibitors, we added the same (5 μM) concentrations of Congo red or rifampicin to the subphase. The area of each monolayer was monitored for 1–4 h.

2.4. Brewster angle microscopy (BAM) and polarised light microscopy

A microscope with laser optics (Nanofilm Technologie, Göttingen, Germany) was assembled near the microbalance (compressed) end of the Langmuir trough to monitor reflection from the Langmuir film [16]. A PC-controlled 10× video recorded any changes including monolayer-associated aggregates or other interesting features. Because such features were spread non-uniformly across the surface, at the conclusion of each experiment we closed the trough barrier to bring any features into the field of view of the microscope. Green birefringence of IAPP samples following the formation of amyloid in the presence or absence of inhibitors was observed in the presence of Congo red using a conventional light microscope equipped with crossed polarising filters.

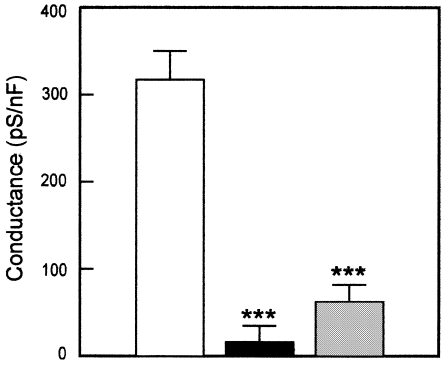

Fig. 1. Rifampicin and Congo red inhibit the membrane activity of IAPP. Planar bilayers that had been stable for 14 min were exposed to 2 μM IAPP by stirring a freshly prepared concentrated solution of the peptide into the *cis* chamber for 1 min. Membrane conductance and capacitance were measured after a further 5 min for control, non-inhibitor treated membranes (open bar), and for membranes exposed to 10 μM rifampicin (black bar) or 10 μM Congo red (grey bar). Data are shown ±S.D. for four to six independent experiments (*** indicates $P < 0.001$ by *t*-testing for significant differences from the control).

3. Results

3.1. Inhibition of IAPP activity in bilayers

Low ionic strength solutions enhance the interaction of IAPP with membranes [8,9], and bilayers were cast in 10 mM KCl containing 20 mM Tris–HCl (pH 7.4) to maximise the effect of IAPP and conserve material. Initially, freshly dissolved IAPP (known to be non-fibrillar, see Section 2) was added to a final concentration of 2 μM to the *cis* side of bilayer membranes that had been shown to be stable for 14 min. IAPP induced a significant increase in membrane conductance when this was re-measured 5 min later (Fig. 1, open bar).

'Channel-like' activity was often visible at early stages of this process, as previously observed [8]. The 'channel-like' activity was more easily visualised by increasing the concentration of the permeant salt to 250 mM (not shown), but the putative channels did not always exhibit well-defined unit conductances, and could not be distinguished from the non-specific electrical leak also known to be induced by the peptide [9]. We therefore calculated macroscopic bilayer conductances, normalised to the bilayer area (i.e. to the bilayer capacitance), and did not attempt to distinguish between 'ion channels' and less well-defined membrane leakiness. As previously reported [9], fibrillar IAPP was ineffective. More prolonged exposure to freshly dissolved IAPP (up to ~15 min) resulted in bilayer instability and breakage (also as previously reported [9]).

The conductance of bilayers exposed to 2 μM freshly dissolved, monomeric [9] IAPP was significantly reduced in the presence of 10 μM rifampicin or 10 μM Congo red (Fig. 1, shaded bars). Rifampicin was more effective than Congo red, and the membrane activity of 5 μM IAPP was reduced in a dose-dependent manner in the presence of rifampicin (Fig. 2), with half-maximal inhibition by 2.9 μM. To determine whether rifampicin could affect the interaction of IAPP with membranes once it had been initiated, 10 μM rifampicin, or vehicle alone (DMSO), was added to membranes 5 min after adding 2 μM IAPP. Before adding the inhibitor, the mem-

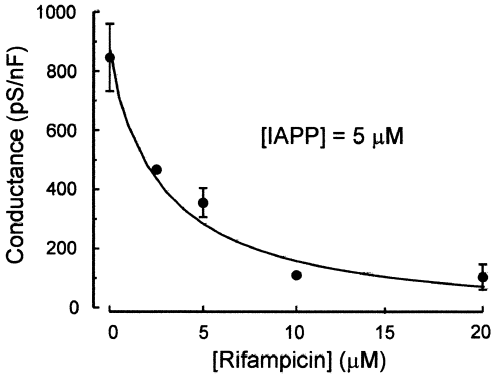

Fig. 2. Inhibition by rifampicin is concentration-dependent. Bilayers formed 14 min earlier were exposed to 5 μM IAPP in the presence of the indicated concentrations of rifampicin. Bars represent ±S.D. of four to five independent experiments, and other points are averages of up to three experiments. The smooth curve is fitted to a single-site inhibition model: conductance = maximum conductance/(1+[rifampicin]/K_i), where K_i is 2.9 μM and maximum conductance = 850 pS/nF.

brane conductance was found to increase with time following IAPP addition, and all the membranes became unstable and broke within 15 min. After the addition of rifampicin, membrane conductances remained elevated, without any evidence that the effect of IAPP was reversed. However, these membranes were 'stabilised', so that their conductance no longer increased with time, and bilayer lifetimes were increased (Fig. 3).

3.2. Inhibition of IAPP activity in monolayers

There are many possible mechanisms by which rifampicin and Congo red could inhibit the membrane activity of IAPP. To investigate the mechanisms in more detail, we constructed classical monocomponent monolayers containing only DMPC, and monolayers containing 1:1 molar mixtures of POPE and POPS, as used for the bilayer experiments. The monolayers were exposed to freshly dissolved IAPP in the presence and absence of inhibitors to determine whether the compounds prevented membrane insertion of the peptide (Fig. 4). Following the injection of 5 μM IAPP into the subphase in the absence of inhibitors, the area of the monolayer expanded substantially with time. The rate of expansion was approximately hyperbolic (Fig. 4, upper trace), and expansion continued for at least 4 h (the maximum period of observation). Control monolayers showed no change in surface area over similar time periods (not shown).

In striking contrast, the surface area of monolayers exposed to IAPP in the presence of 5 μM rifampicin failed to increase (Fig. 4, lower trace), indicating that under these conditions the peptide remained confined to the subphase, and did not interact with the lipid monolayer. The initial rate of IAPP-induced increase in surface area was reduced when the subphase contained 5 μM Congo red, but thereafter monolayer expansion continued at about the same rate seen in IAPP-exposed monolayers. In the experiment shown in Fig. 4 (middle trace), the monolayer expanded (over 60 min) to 93 Å^2 per molecule of pure lipid in the presence of Congo red, compared to 103 Å^2 per molecule of pure lipid without inhibitor (itself representing a 60% increase in area compared to control membranes). We obtained similar results using DMPC monolayers (results not shown).

Complementary BAM observations, making use of the unique (Brewster) angle of incidence that just disallows surface reflections under control conditions, permitted highly sensitive observations of optical changes at the monolayer/subphase interface following the addition of IAPP [16]. We observed pleomorphic changes as IAPP associated with monolayers, including extensive, irregular surface-associated structures containing regions of very bright reflection (Fig. 5). Although monolayers exposed to IAPP in the presence of Congo red also developed extensive surface-associated deposits of IAPP, none of these changes was seen in the presence of rifampicin. Finally, we confirmed that IAPP pre- or post-stained with Congo red formed birefringent aggregates typical of amyloid deposits over the course of 24–48 h when viewed under crossed polarisers (not shown), even when IAPP was

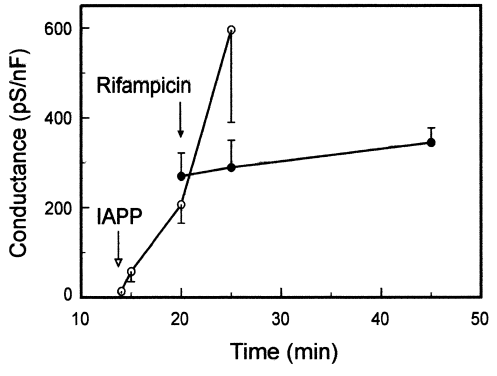

Fig. 3. Rifampicin 'stabilises' planar bilayers exposed to IAPP. 2 μM IAPP was added to bilayers that had been stable for after 14 min, and stirred in for 1 min. The membrane conductance was measured at intervals (open symbols) up to 25 min (i.e. 11 min after IAPP addition). After this time, up to 50% of the bilayers broke. In some experiments, 10 μM rifampicin was added 6 min after IAPP (filled symbols). These bilayers remained intact, and measurements were continued for a further 25 min without bilayer breakdown. Bars indicate ±S.E.M. for three to five independent experiments.

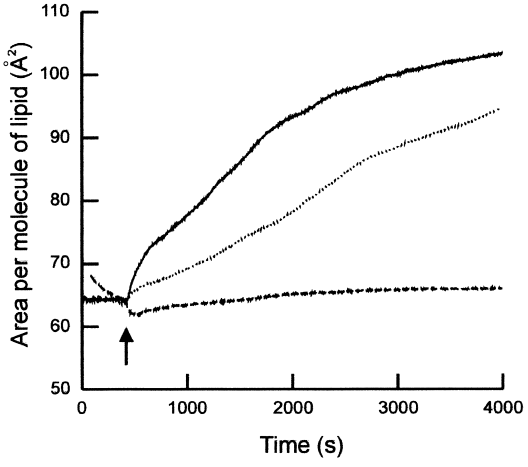

Fig. 4. Inhibitors attenuate or arrest IAPP-induced monolayer expansion. Representative traces from three experiments recording monolayer expansion (at constant surface pressure) after adding 5 μM IAPP to the subphase (arrow) in the absence of inhibitors (upper trace, continuous line), in the presence of 5 μM Congo red (middle trace, dotted line), and in the presence of 5 μM rifampicin (lower trace, broken line). The monolayer contained equimolar POPE:POPS. Similar results were obtained using DMPC (not shown).

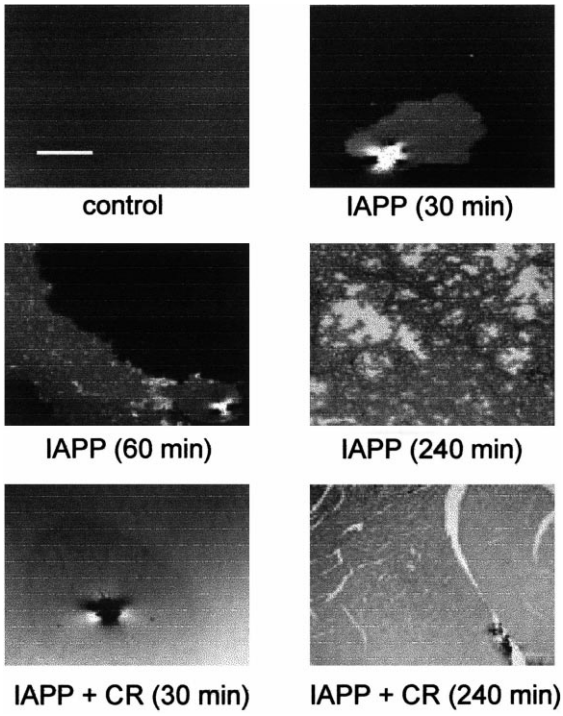

Fig. 5. IAPP-induced changes in membrane reflection visualised by BAM. Representative BAM images showing appearances at the monolayer/water interface in control DMPC monolayers, which showed no change in appearance with time, and monolayers exposed to 5 μM IAPP in the presence and absence of 5 μM Congo red (CR). Times refer to minutes after IAPP addition. The scale bar (control monolayer) represents 100 μm, and applies to all the images.

exposed to 5 μM of the inhibitors immediately from the outset of solubilisation.

4. Discussion

Rifampicin prevented amyloidogenic, membrane-active IAPP from increasing the conductance of planar lipid bilayers. Although Congo red was less protective (at the same concentration), it also reduced membrane activity significantly. Rifampicin also 'stabilised' bilayer membranes, so that membrane lifetimes were no longer markedly reduced in the presence of the membrane-active peptide. However, neither rifampicin nor Congo red prevented the time-dependent assembly of IAPP into amyloid fibrils showing diagnostic green birefringence when stained with Congo red. Studies using lipid monolayers indicated that rifampicin prevents the membrane incorporation of IAPP, but compared to rifampicin, similar concentrations of Congo red only partially inhibited the interaction of IAPP with both neutral and charged monolayers.

Although IAPP [8] (and other amyloidogenic proteins, e.g. Aβ [17]) have been shown to give rise to 'channel-like' activity in bilayers, we did not observe well-defined unit conductances in the present study, suggesting that IAPP-related transmembrane ion channels may not have a consistent, well-defined molecular structure. Also, the formation of discrete ion channels cannot explain the membrane instability and breakage associated with IAPP. In these respects, the membrane activity of IAPP resembles that of the soluble, apoptosis-related proteins that induce pore formation in mitochondrial membranes, especially Bax [18]. Basanez et al. [18] provided evidence to support the idea that Bax-induced ion channels contain intercalated lipid, helping to explain why Bax-mediated pores enlarge uncontrollably beyond a certain critical diameter. In addition to the uncertainties concerning the molecular structure of membrane channels or leak pathways induced by amyloidogenic membrane-active proteins, the mechanism by which the proteins actually become incorporated into membranes also remains unclear. We speculated that the inhibitors might affect the membrane insertion of IAPP, and we attempted to gain insights into this and other aspects of the membrane activity of IAPP by carrying out experiments involving lipid monolayers (Langmuir films).

Despite very obvious structural differences, lipid monolayers can nevertheless provide useful information about the behaviour of lipid bilayers (the principle of equivalent states [19]). IAPP inserted spontaneously into ultrathin lipid films, inducing large increases in membrane surface area. Under the experimental conditions we used, the surface area increased up to two-fold over the course of $\sim$4 h, with much of this increase taking place within the first 20 min of exposure to IAPP. The rapid intercalation of protein on such a major scale was unexpected, and would be predicted to lead to the membrane disruption commonly observed in bilayers. Equimolar rifampicin completely prevented IAPP insertion, while equimolar Congo red slowed the initial rate of incorporation of IAPP into the monolayer. Using BAM, we observed aggregates of IAPP in or just below the plane of the monolayer. Aggregates were not formed in the presence of rifampicin, suggesting that under the conditions used here, rifampicin completely prevents any interaction between IAPP and the membrane lipids.

Taken together, our results show that IAPP incorporates spontaneously into membranes to form extensive higher order structures. We speculate that the intensely bright regions frequently seen in the IAPP aggregates under BAM represent IAPP-enriched regions where the polypeptide has completely traversed the monolayer to become surface-exposed. The incorporation of membrane-active β-sheet rich proteins into membranes may be enhanced by electrostatic interactions [20], and may be accompanied by a poorly understood structural transition giving rise to transmembrane α-helices [21–23]. It is possible that such transmembrane helices could associate to form water-filled ion channels. Results from monolayer studies clearly cannot be compared directly to bilayers because of the absence of one leaflet of the bilayer, and also because the behaviour of monolayers (especially those containing more than one lipid species) is incompletely characterised [24]. However, monolayer studies appear to have the potential to provide useful information concerning the interaction of IAPP with phospholipids, especially when combined with studies in planar bilayers and experiments on living cells.

Some of our results concerning IAPP may also have implications for AD, where amyloid-containing plaques are comprised of 40–43 residue polypeptides (Aβ1–40, Aβ1–42 and Aβ1–43) produced by proteolytic processing of amyloid precursor protein [25]. Although (as in NIDDM) there is clearly a close relationship between amyloid production and the disease, in AD amyloid deposition is unlikely to be the primary problem. Many other changes occur in AD, including changes that appear to be entirely unrelated to Aβ1–42(3) production,

and it is significant that transgenic animals with fully convincing pathological and behavioural 'AD' phenotypes have yet to be generated. Despite this, it is generally accepted that Aβ peptides, like hIAPP, interact with and disrupt the function of cell membranes. Iversen et al. [25] discuss the strong circumstantial evidence linking Aβ proteins to a causative role in AD, and in vitro these peptides also form Ca^{2+}-permeable ion channels [17], similar to hIAPP. Prion proteins are also amyloidogenic, and bind to membranes [26]. Recombinant antibody antigen-binding fragments that inhibit prion propagation appear to act on cell surface prions [27], and it will be interesting to discover whether the recently described antiprion pharmacotherapeutics of Korth et al. [28] act in a related manner.

The structural basis underlying the interactions of rifampicin and Congo red with IAPP, leading to the modification of its membrane activity, remains to be determined. The inhibitors appear to associate with IAPP to prevent or modify membrane incorporation, but several molecular mechanisms may be involved. Future studies using model membranes will help to define these mechanisms, and may identify additional compounds that also prevent (or reverse) IAPP-induced membrane damage. Small molecule therapeutics may provide a novel approach to disable membrane-active IAPP (or Aβ) in NIDDM (or AD), irrespective of whether the fundamental biological mechanism is related to defective molecular chaperoning or to other defects in protein processing in β cells or neurones. Inhibitors of the membrane activity of IAPP may also stabilise membrane-associated complexes, to facilitate detailed structural analysis.

Acknowledgements: We thank Arwel Hughes and Steve Roser (Department of Chemistry, University of Bath, Bath, UK) for advice on Langmuir trough experiments. This work was supported by the Wellcome Trust.

References

[1] Goldsbury, C.S., Cooper, G.J.S., Goldie, K.N., Muller, S.A., Saafi, E.L., Gruijters, W.T.M., Misur, M.P., Engel, A., Aebi, U. and Kistler, J. (1997) J. Struct. Biol. 119, 17–27.
[2] Pauling, L. and Corey, R. (1951) Proc. Natl. Acad. Sci. USA 37, 729–739.
[3] De Lellis, R.A., Glenner, G.G. and Ram, J.S. (1968) J. Histochem. Cytochem. 16, 663–665.
[4] Li, L., Darden, T.A., Bartolotti, L., Kominos, D. and Pedersen, L.G. (1999) Biophys. J. 76, 2871–2878.
[5] Westermark, P., Engstrom, U., Johnson, K.H., Westermark, G.T. and Betsholz, C. (1990) Proc. Natl. Acad. Sci. USA 87, 5036–5040.
[6] Tenidis, K., Waldner, M., Bernhagen, J., Fischle, W., Bergmann, M., Weber, M., Merkle, M.-L., Voelter, W., Brunner, H. and Kapurniotu, A. (2000) J. Mol. Biol. 295, 1055–1071.
[7] Janson, J., Soeller, W.C., Roche, P.C., Nelson, R.T., Torchia, A.J., Kruetter, D.K. and Butler, P.C. (1996) Proc. Natl. Acad. Sci. USA 9, 7283–7288.
[8] Mirzabekov, T.A., Lin, M.C. and Kagan, B.L. (1996) J. Biol. Chem. 271, 1988–1992.
[9] Janson, J., Ashley, R.H., Harrison, D., Butler, P.C. and McIntyre, S. (1999) Diabetes 48, 491–498.
[10] Davis-Salinas, J. and Van Nostrand, W.E. (1995) J. Biol. Chem. 270, 20887–20890.
[11] Tomiyama, T., Soji, A., Kataoka, K., Suwa, Y., Asano, S., Kaneko, H. and Endo, N. (1996) J. Biol. Chem. 271, 6839–6844.
[12] Tomiyama, T., Kaneko, H., Kataoka, K., Asano, S. and Endo, N. (1997) Biochem. J. 322, 859–865.
[13] Burgevin, M.C., Passat, M., Daniel, N., Capet, M. and Doble, A. (1994) NeuroReport 5, 2429–2432.
[14] Lorenzo, A. and Yankner, B.A. (1996) Ann. N.Y. Acad. Sci. 777, 89–95.
[15] Williams, A.J. (1995) in: Ion Channels, a Practical Approach (Ashley, R.H., Ed.), pp. 43–67, IRL/OUP, Oxford.
[16] Kozarac, Z., Dhathathreyan, A. and Mobius, D. (1987) Eur. Biophys. J. 15, 193–196.
[17] Pollard, H.B., Arispe, N. and Rojas, E. (1995) Cell. Mol. Neurobiol. 15, 513–526.
[18] Basanez, G., Nechushtan, A., Drozhinin, O., Chanturiya, A., Choe, E., Tutt, S., Wood, K.A., Hsu, Y., Zimmerberg, J. and Youle, R.J. (1999) Proc. Natl. Acad. Sci. USA 96, 5462–5497.
[19] Peterson, I.R. (1994) Langmuir 10, 4645–4650.
[20] Hertel, C., Terzi, E., Hauser, N., Jacob-Rotne, R., Seelig, J. and Kemp, J.A. (1997) Proc. Natl. Acad. Sci. USA 94, 9412–9416.
[21] Bradshaw, J.P. (1997) Biophys. J. 72, 2180–2186.
[22] McLaurin, J. and Chakrabartty, A. (1997) Eur. J. Biochem. 245, 355–363.
[23] Zhang, S.G. and Rich, A. (1997) Proc. Natl. Acad. Sci. USA 94, 23–28.
[24] Johnston, D.S., Coppard, E. and Chapman, D. (1985) Biochim. Biophys. Acta 815, 325–333.
[25] Iversen, L.L., Mortishire-Smith, R.J., Pollack, S.L. and Shearman, M.S. (1995) Biochem. J. 311, 1–16.
[26] Rymer, D.L. and Good, T.A. (2000) J. Neurochem. 75, 2536–2545.
[27] Peretz, D., Williamson, D.A., Kaneko, K., Vergara, J., Leclerc, E., Schmitt-Ulms, G., Mehihorn, I.R., Legname, G., Wormald, M.R., Rudd, P.M., Dwek, R.A., Burton, D.R. and Prusiner, S.B. (2001) Nature 412, 739–743.
[28] Korth, C., May, B.C.H., Cohen, F.E. and Prusiner, S.B. (2001) Proc. Natl. Acad. Sci. USA 98, 9836–9841.